Development of a New Method for Synthesis of Tandem Hairpin Pyrrole−Imidazole Polyamide Probes Targeting Human Telomeres

Yusuke Kawamoto,[†] Toshikazu Bando,*[,†] Fukumi Kamada,[‡] Yue Li,[†] Kaori Hashiya,[†] Kazuhiro Maeshima,*[,‡,§] and Hiroshi Sugiyama*[,†,∥,⊥]

[†]Department of Chemistry, Graduate School of Science, Kyoto University, Sakyo, Kyoto 606-8502, Japan

[‡]Biological Macromolecules Laboratory, Structural Biology Center, National Institute of Genetics, Mishima, Shizuoka 411-8540, Japan

[§]Department of Genetics, School of Life Science, Graduate University for Advanced Studies (Sokendai), Mishima, Shizuoka 411-8540, Japan

[∥]Institute for Integrated Cell-Material Science (WPI-iCeMS), Kyoto University, Sakyo, Kyoto 606-8501, Japan

[⊥]Core Research for Evolutional Science and Technology (CREST), Japan Science and Technology Corporation (JST), Sanbancho, Chiyoda-ku, Tokyo 102-0075, Japan

S Supporting Information

ABSTRACT: Pyrrole−imidazole (PI) polyamides bind to the minor groove of DNA in a sequence-specific manner without causing denaturation of DNA. To visualize telomeres specifically, tandem hairpin PI polyamides conjugated with a fluorescent dye have been synthesized, but the study of telomeres using these PI polyamides has not been reported because of difficulties synthesizing these tandem hairpin PI polyamides. To synthesize tandem hairpin PI polyamides more easily, we have developed new PI polyamide fragments and have used them as units in Fmoc solid-phase peptide synthesis. Using this new method, we synthesized four fluorescent polyamide probes for the human telomeric repeat TTAGGG, and we examined the binding affinities and specificities of the tandem hairpin PI polyamides, the UV−vis absorption and fluorescence spectra of the fluorescent polyamide probes, and telomere staining in mouse MC12 and human HeLa cells. The polyamides synthesized using the new method successfully targeted to human and mouse telomeres under mild conditions and allow easier labeling of telomeres in the cells while maintaining the telomere structure. Using the fluorescent polyamides, we demonstrated that the telomere length at a single telomere level is related to the abundance of TRF1 protein, a shelterin complex component in the telomere.

INTRODUCTION

Telomeres locate to the end of chromosomes and are important to the stability and replication of chromosomes.[1] The human telomeric DNA consists of a very long duplex region of the 5′-TTAGGG-3′ sequence with a 3′ overhang and single strands that tend to form G-quadruplexes or t-loops.[2] Vertebrates including humans have the repetitive sequence TTAGGG as telomeres.[1] In normal mammalian cells, the number of telomere repeats decreases with cell division, relating to aging process.[3,4] The telomere length is regulated by a shelterin complex including TRF1, TRF2, Rap1, TIN2, TPP1, and POT1 and is one important biomarker used in various diagnoses.[2−5] Therefore, the design and synthesis of fluorescently labeled polyamides, which target telomeres, have attracted strong interest for visualization and measurement of telomere length.

Dervan and co-workers demonstrated that N-methylpyrrole (P)−N-methylimidazole (I) (PI) polyamides bind to the minor groove of duplex DNA without causing denaturation of dsDNA and can recognize Watson−Crick base pairs.[6] An antiparallel pairing of I opposite P (I−P) recognizes a G·C base pair,

whereas a P−P pair recognizes an A·T or T·A base pair.[7] For efficient binding to long sequences, β-alanine residues are introduced to adjust the pitch of the DNA base pairs and to act as an aliphatic substitution for a P ring.[8] PI polyamides have strong binding affinity and sequence selectivity that can be used for targeting DNA sequences. To date, various structures of PI polyamides have been developed, such as hairpin,[9] cyclic,[10] and tandem hairpin.[11,12] These have been used as sequence-specific alkylating agents,[13] fluorescent probes,[14] and SAHA conjugates[15] and for other uses.

PI polyamides conjugated with fluorescent dyes or alkylating agents have been developed for observing telomeres and studying their influence on the proliferation of cancer cells. Our laboratory has developed fluorescent probes[16] and alkylating agents[17] that target human telomere sequences. Maeshima, Janssen, and Laemmli reported PI polyamide probes that can bind strongly to the human telomeric repetitive sequence
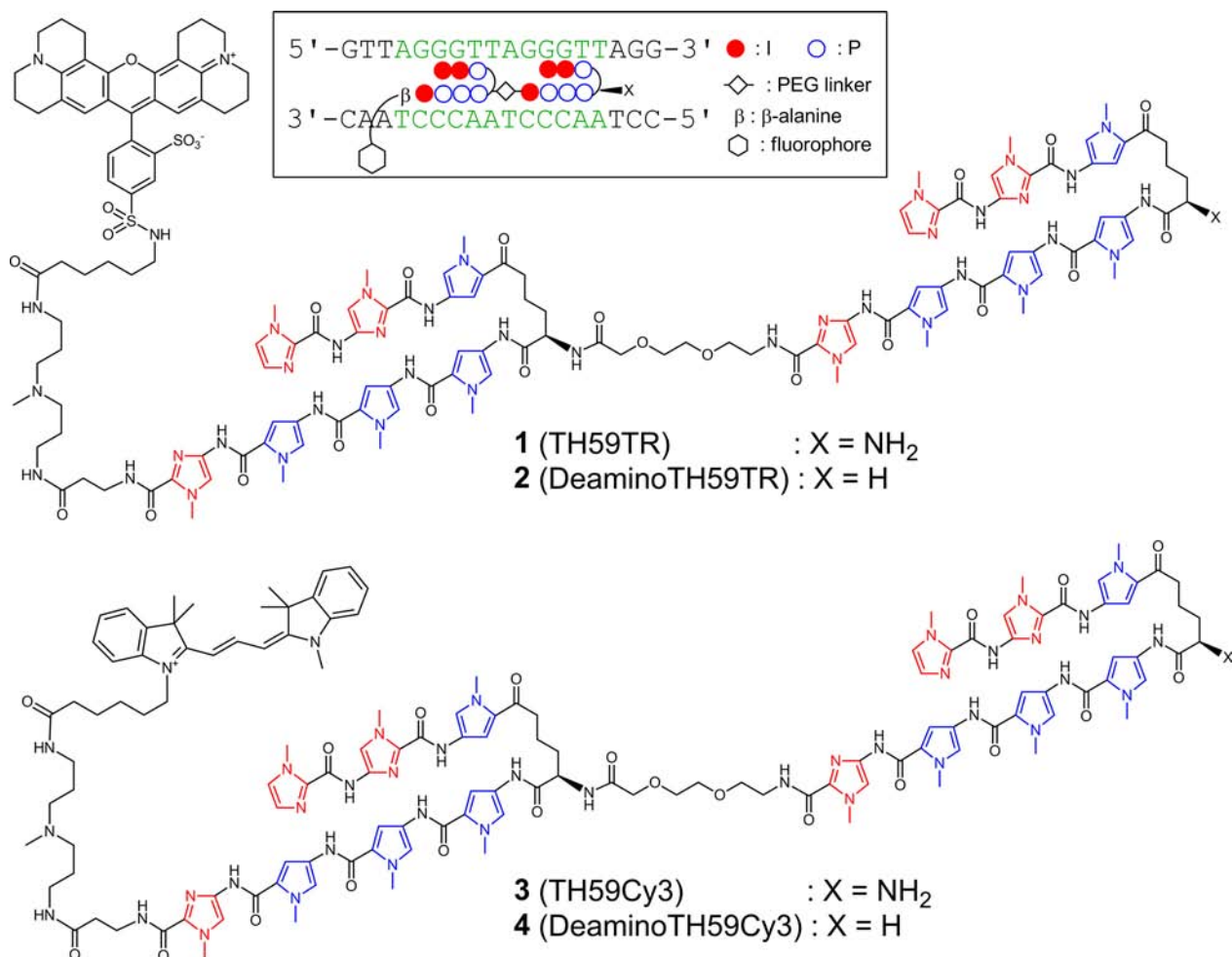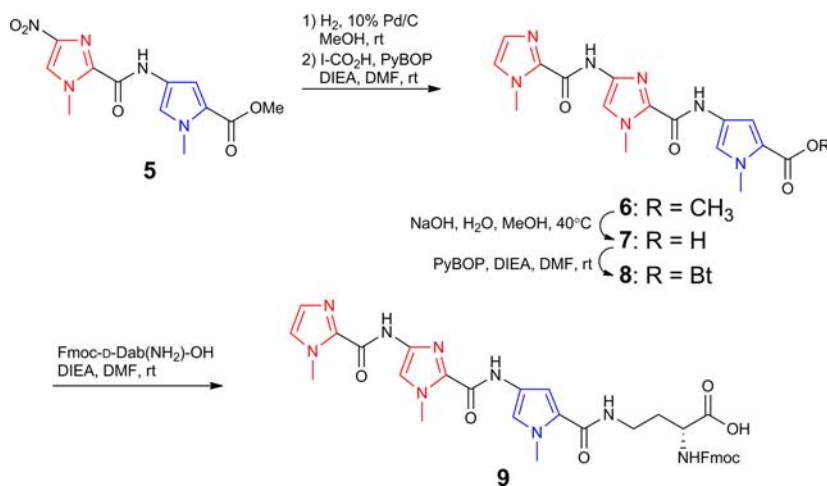
Figure 1. Chemical structure of tandem hairpin fluorescent PI polyamides **1−4** targeting the human telomere sequence and their ball-and-stick representation.

Scheme 1. Synthesis of PI Polyamide Units 7 and 9 for Solid-phase Synthesis

TTAGGG ($K_D = 0.51$ nM) in the duplex regions and can be used to stain telomeres in chemically fixed cells.[12]

Hairpin PI polyamides with a γ-aminobutyric acid turn (γ-turn) have both sequence specificity and DNA binding affinity,[9] and they can be synthesized easily by machine-assisted Fmoc solid-phase peptide synthesis (SPPS).[18] Tandem hairpin PI polyamides comprise two hairpin PI polyamides linked with a

flexible linker and can recognize ≥10 base pairs.[11,12] However, the yield of tandem hairpin PI polyamides was low because multiple steps were needed to remove Boc groups or Fmoc groups in Fmoc SPPS or Boc SPPS, respectively. Therefore, the interruption of automatic coupling reactions for the deprotection of amino groups was needed.[11a,b,d] The detailed

Scheme 2. Solid-Phase Synthesis of Tandem Hairpin Fluorescent PI Polyamides 1−4[a]
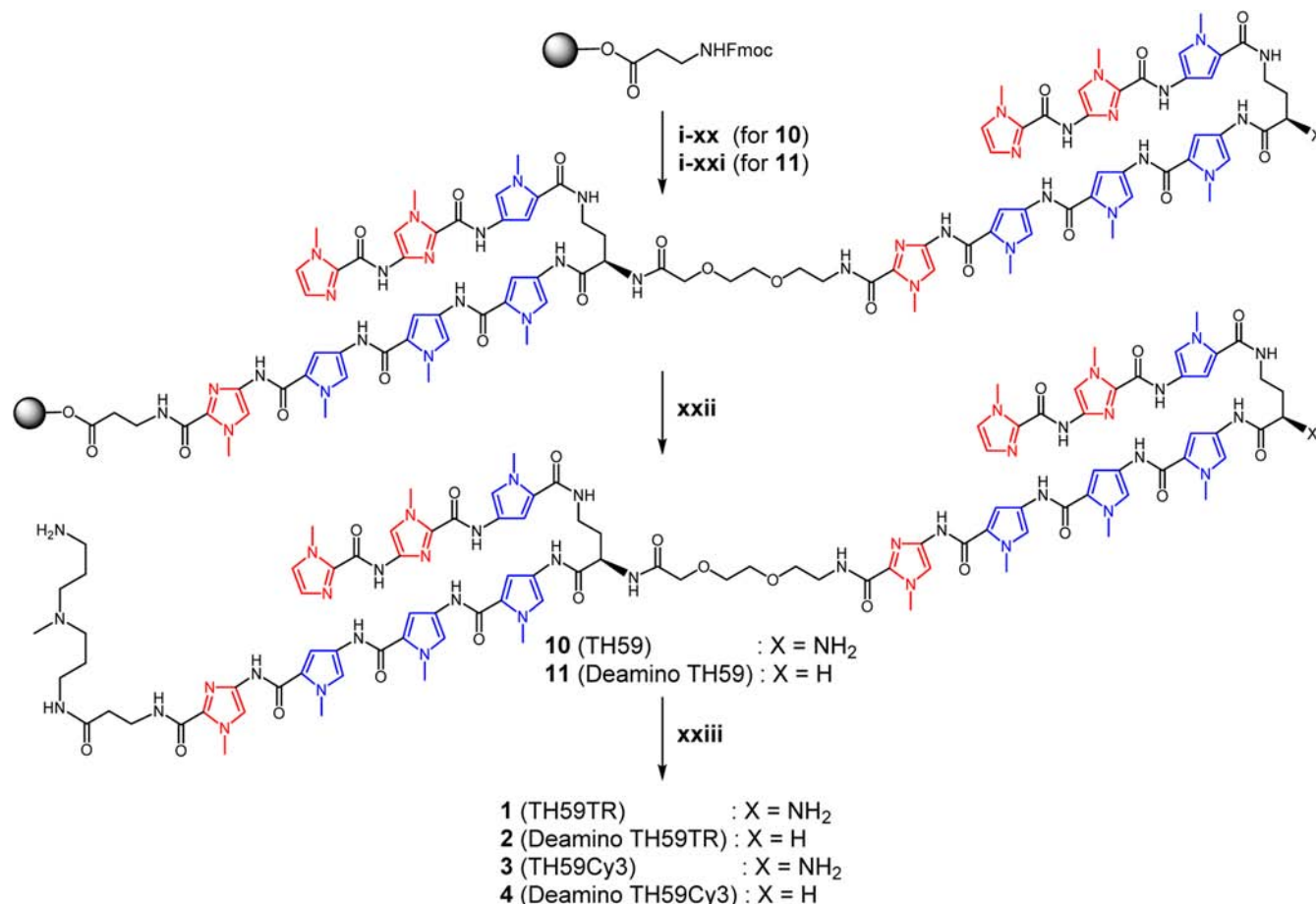
[a]All HCTU-mediated coupling conditions were performed under similar conditions (see ref 10c). Reagents and conditions: (i) 20% piperidine, DMF; (ii) Fmoc-PI-CO₂H, HCTU, DIEA, DMF; (iii) 20% piperidine, DMF; (iv) Fmoc-P-CO₂H, HCTU, DIEA, DMF; (v) 20% piperidine, DMF; (vi) Fmoc-P-CO₂H, HCTU, DIEA, DMF; (vii) 20% piperidine, DMF; (viii) **9**, HCTU, DIEA, DMF; (ix) 20% piperidine, DMF; (x) Fmoc-mini-PEG-OH, HCTU, DIEA, DMF; (xi) 20% piperidine, DMF; (xii) Fmoc-PI-CO₂H, HCTU, DIEA, DMF; (xiii) 20% piperidine, DMF; (xiv) Fmoc-P-CO₂H, HCTU, DIEA, DMF; (xv) 20% piperidine, DMF; (xvi) Fmoc-P-CO₂H, HCTU, DIEA, DMF; (xvii) 20% piperidine, DMF; (xviii) **9**, HCTU, DIEA, DMF (for **10**) or Fmoc-γ-Abu−OH, HCTU, DIEA, DMF (for **11**) ; (xix) 20% piperidine, DMF; (xx) **7**, PyBOP, DIEA, DMF (for **11**) ; (xxi) 3,3′-diamino-*N*-methyldipropylamine, 45 °C; (xxii) TR succinimidyl ester, DIEA, DMF (for **1** and **2** from **10** and **11**, respectively) or Cy3-NHS ester, DIEA, DMF (for **3** and **4** from **10** and **11**, respectively).

synthetic protocols for some polyamides have not been described.[12]

To overcome the difficulties associated with the synthesis of tandem hairpin PI polyamides, we herein demonstrate a new synthetic route for creating tandem hairpin PI polyamides in which the tetraamide unit, **9**, synthesized in the solution phase, is introduced into Fmoc SPPS. Using this method, we synthesized four polyamide−fluorescent probes conjugated with Texas Red (TR) or Cyanine 3 (Cy3) to visualize mammalian telomeres. This new synthetic route is more efficient and applicable to a wider variety of tandem hairpin PI polyamides compared with the methods reported previously because machine-assisted SPPS without any interruptions can provide tandem hairpin PI polyamides. Thermal denaturation analysis ensured their binding to and specificities for human telomeric repetitive sequence. The synthesized fluorescent polyamide probe conjugates were evaluated by measuring the UV−vis absorption and fluorescence intensity and by telomere staining of the polyamides in mouse and human cells. This new method simplifies the synthesis of tandem hairpin PI

polyamides and also the observation of human telomeres using these PI polyamide−fluorescent probes.

■ RESULTS AND DISCUSSION

Synthesis of Conjugates 1−4. To synthesize the conjugates **1−4** (Figure 1), we synthesized the new tetraamide unit **9** (Scheme 1). Reduction of the compound **5**, synthesized using the previous method,[13a] was performed under high pressure (0.23 MPa) of hydrogen gas with 10% Pd/C to afford amine crude powder, which was coupled with 1-methyl-1*H*-imidazole-2-carboxylic acid using benzotriazol-1-yloxytripyrrolidinophosphonium hexafluorophosphate (PyBOP) and *N,N*-diisopropylethylamine (DIEA) in *N,N*-dimethylformamide (DMF) to produce the compound **6**. The crude compound **6** was hydrolyzed to obtain the first key compound **7**. Next, the crude compound **7** was activated with PyBOP to afford the compound **8**, followed by coupling with the deblocked Fmoc-D-Dab(Boc)-OH to produce the second key compound **9**. The crude compound **9** was washed with diethyl ether and then triturated with water. Using the compounds **7** and **9** as units without further purification, machine-assisted solid-phase
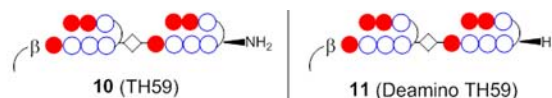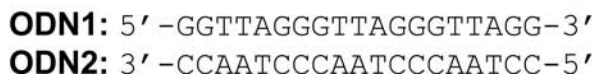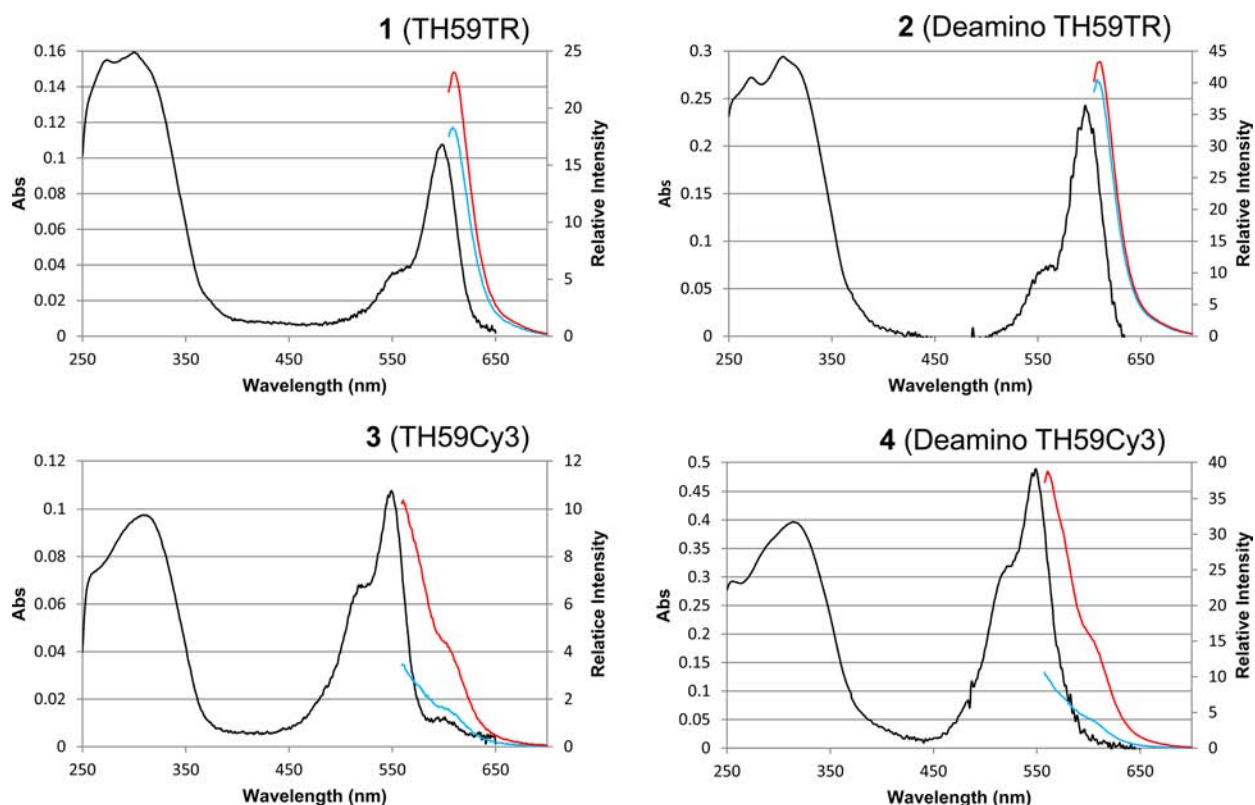
ODN1: 5'-GGTTAGGGTTAGGGTTAGG-3'
ODN2: 3'-CCAATCCCAATCCCAATCC-5'

Figure 2. UV−vis absorption spectra (black) of conjugates **1**−**4** ([**1**] = [**2**] = [**3**] = [**4**] = 6 μM) in a 5 mM Na phosphate buffer (pH 7.0, **1** and **3** containing 10% v/v DMF, **2** and **4** containing 3% v/v DMF) and fluorescence emission spectra of conjugates **1**−**4** (3 μM) in the absence of ODN-1/2 (blue) or presence of 6 μM ODN-1/2 (red) in 5 mM Na phosphate buffer (pH 7.0 containing 5% v/v DMF).

peptide synthesis shown in Scheme 2 was performed to afford the tandem hairpin PI polyamides **10** (named TH59[12]) and **11** (named deamino TH59). The compound **11**, which does not have an amino group at the γ-turn, was designed for the ease of synthesis of tandem hairpin PI polyamides. The new units **7** and **9** allowed us to omit the steps to remove Boc groups on the resin and to synthesize tandem hairpin PI polyamides automatically and easily. The crude tandem hairpin PI polyamides **10** and **11** were cleaved from the resin using 3, 3′-diamino-*N*-methyldipropylamine and then purified by reversed-phase flash chromatography, followed by coupling with TR succinimidyl ester or Cy3-NHS ester in DMF and DIEA to afford conjugates **1**−**4** (TH59TR, deamino TH59TR, TH59Cy3, deamino TH59Cy3, respectively) after purification by reversed-phase HPLC (Scheme 2). ESI-TOF MS spectra of **1**−**4**, **10**, and **11** are shown in Figures S1,2, Supporting Information.

UV−vis Absorption Spectra and Fluorescence Spectra. The UV−vis absorption and fluorescence spectra of conjugates **1**−**4** are shown in Figure 2. The absorption spectra (black lines) of conjugates **1**−**4** were measured at the same concentration (6 μM) in 5 mM Na phosphate buffer (pH 7.0; **1** and **3** containing 10% v/v DMF, **2** and **4** containing 3% v/v DMF). The absorption maximum due to the dye of **1** and **2**, which were conjugated with TR, was 596 nm, and that of **3** and **4**, conjugated with Cy3, was 549 nm. These maxima were mostly consistent with each dye's excitation wavelength.[14a] The

absorption maximum at ∼310 nm was due to the pyrrole and imidazole moieties.

The fluorescence spectra of conjugates **1**−**4** (3 μM) in 5 mM Na phosphate buffer (pH 7.0 containing 5% v/v DMF) in the absence and presence of oligonucleotide (ODN)-1/2, whose sequences were 5′-GGTTAGGGTTAGGGTTAGG-3′ (ODN-1) and 3′-CCAATCCCAATCCCAATCC-5′ (ODN-2), are shown in Figure 2 by blue and red lines, respectively. In each case, addition of ODN-1/2 provided stronger emission, but compounds **1** and **2** having an emission maximum at 609 nm (λ_{ex} = 596 nm) differed slightly between the absence and presence of ODN-1/2 (1.3-fold and 1.1-fold greater, respectively). By contrast, the emission maxima at 560 nm (λ_{ex} = 549 nm) of **3** and **4** were 3.0-fold and 3.9-fold greater with than without ODN-1/2, respectively. Similar enhancement of the fluorescence of tetramethylrhodamine (TMR) and perylene by addition of dsDNA was reported by Dervan and co-workers[19] and our laboratory,[16] respectively. It was suggested that hydrophobic intramolecular interactions between the TMR and the polyamide formed in the absence of dsDNA would induce electron transfer from the polyamide to the singlet excited state of the TMR and the fluorescence would be quenched, and this interaction would be disrupted in the presence of matched dsDNA, resulting in an increase in fluorescence.[19b] The changes in fluorescence of the polyamide−Cy3 conjugates may occur presumably because of this quenching, and therefore this system may not be applied to the polyamide−TR conjugates.

Table 1. T_m Values for Tandem Hairpin PI Polyamides 10 and 11[a]

dsDNA sequences targeted by polyamides	10 (TH59)			11 (Deamino TH59)		
	T_m	ΔT_m	ΔT_m(match)-ΔT_m(mismatch)	T_m	ΔT_m	ΔT_m(match)-ΔT_m(mismatch)
Match DNA (T_m: 43.7°C (±0.4°C)) 5′- GGTT**AGGGTTAGGGTT**AGG -3′ 3′- CCAA**TCCCAATCCCAA**TCC -5′	69.7°C (±0.5°C)	26.0°C	—	62.8°C (±0.3°C)	19.1°C	—
1 bp Mismatch DNA (T_m: 44.5°C (±0.5°C)) 5′- GGTT**AGAGTTAGGGTT**AGG -3′ 3′- CCAA**TCTCAATCCCAA**TCC -5′	62.8°C (±0.2°C)	18.3°C	7.6°C	56.7°C (±0.7°C)	12.2°C	6.9°C
1 bp Mismatch DNA (T_m: 44.6°C (±0.5°C)) 5′- GGTT**AGGGTTAGAGTT**AGG -3′ 3′- CCAA**TCCCAATCTCAA**TCC -5′	63.3°C (±0.2°C)	18.8°C	7.2°C	57.6°C (±0.2°C)	13.0°C	6.1°C
2 bp Mismatch DNA (T_m: 43.4°C (±0.3°C)) 5′- GGTT**AGAGTTAGAGTT**AGG -3′ 3′- CCAA**TCTCAATCTCAA**TCC -5′	55.1°C (±0.3°C)	11.7°C	14.3°C	49.3°C (±0.3°C)	5.9°C	13.3°C

[a]All T_m values are the average calculated from at least four melting temperature analyses with standard deviations indicated in parentheses. ΔT_m values are given as T_m(polyamide−DNA complex) − T_m(DNA).

Binding Affinities and Specificities of Tandem Hairpin PI Polyamides. Thermal stabilization of polyamide−DNA complex can be analyzed by thermal melting temperature (T_m) analysis, and this method has been used for the measurement of the relative binding affinity and the ability to discriminate mismatch sequences.[20] In order to confirm whether tandem hairpin PI polyamides 10 (TH59) and 11 (deamino TH59) bind to telomeric repeats strongly and specifically, thermal denaturation analysis of DNA and of polyamides−DNA complex was performed. The sequences of dsDNA were 5′-GGTTAGGGTTAGGGTTAGG-3′ (ODN-1) and 3′-CCA-ATCCCAATCCCAATCC-5′ (ODN-2), 5′-GGTTAGAGTT-AGGGTTAGG-3′ (ODN-3) and 3′-CCAATCTCAATCC-CAATCC-5′ (ODN-4), 5′-GGTTAGGGTTAGAGTTAGG-3′ (ODN-5) and 3′-CCAATCCCAATCTCAATCC-5′ (ODN-6), and 5′-GGTTAGAGTTAGAGTTAGG-3′ (ODN-7) and 3′-CCAATCTCAATCTCAATCC-5′ (ODN-8), which had no mismatch, 1 bp mismatch at the side of the polyamides' C-termini, l bp mismatch at the side of their N-termini, and 2 bp mismatch, respectively. The underlined bases are the binding sites of polyamides, and the bold bases show mismatched parts. The analysis buffer is the aqueous solution of 10 mM sodium chloride and 10 mM sodium cacodylate at pH 7.0 containing 2.5% v/v DMF. The concentration of polyamides and dsDNA was 12.5 and 2.5 μM, respectively (5:1 stoichiometry). When analyzing in other stoichiometry (1:1, and 2:1), reasonable melting transition at a stoichiometry of 1:1 and 2:1 was not observed (data not shown). There is an example of the UV thermal denaturation profile of DNA duplexes in the presence of DNA binder targeting 10−12 bp at 5 mol equivalent or higher.[21] Before analyses, samples were annealed from 80 °C to room temperature for 1 h. Denaturation profiles were recorded at λ= 260 nm from 25 to 90 °C at a rate of 1.0 °C/min and are shown in Figures S3−6, Supporting Information. The resulting values are shown in Table 1. The ΔT_m values of 10-ODN-1/2 and 11-ODN-1/2 were 26.0 and 19.1 °C, respectively, demonstrating that these tandem hairpin PI polyamides can bind to TTAGGG repeats and, especially, the affinity of 10 was equivalent to cyclic PI polyamides, which have high binding affinities (i.e., ΔT_m > 20.0 °C).[10a,d] Compound 10 has the higher affinity than 11 presumably because of the amino group at the γ-turn.[22] ΔT_m(match) − ΔT_m(mismatch) ($\Delta\Delta T_m$) values of 10-ODN-3/4 and 11-ODN-3/4 were 7.6 and 6.9 °C, respectively. In

contrast, $\Delta\Delta T_m$ values of 10-ODN-5/6 and 11-ODN-5/6 were 7.2 and 6.1 °C, respectively. Moreover the complex of 10 and 11 and ODN-7/8, which has 2 bp mismatch, show higher $\Delta\Delta T_m$ values, 14.3 and 13.3 °C, respectively. These results suggests tandem hairpin PI polyamides can discriminate 1 bp and 2 bp mismatch and the hairpin PI polyamides at the side of N-termini have slightly better abilities of the discrimination than those at the side of C-termini.

Telomere Targeting of the Synthesized Fluorescent Polyamides in Mouse and Human Cells. We doubly stained mouse MC12 cell spreads with the fluorescent polyamides and 4′, 6-diamidino-2-phenylindole (DAPI) to compare the ability of conjugates 1−4 (TH59TR, deamino TH59TR, TH59Cy3, deamino TH59Cy3) to stain telomeres specifically. We examined various staining conditions and found that the optimal result was obtained using PI polyamide binding with low-salt washing, followed by higher-salt washing, as described in the Materials and Methods. The images are shown in Figure 3. The DAPI signal shows chromosomal regions. The PI polyamide signals show intense foci, which represent the subchromosomal binding with the polyamides. In each case, two foci are observed at every chromosomal end, suggesting that all TH59TR, deamino TH59TR, TH59Cy3, and deamino TH59Cy3 can bind to the mouse telomeric repeat TTAGGG. The background signals increased when stained with TH59Cy3 and deamino TH59Cy3, whereas little background was detected along chromosomes treated with the TH59TR and deamino TH59TR. This result is presumably because Cy3 induced nonspecific binding of polyamides, but TR did not induce such binding. Although in vitro analysis showed that TH59Cy3 and deamino TH59Cy3 fluoresced more strongly when bound to the targeted DNA (shown in Figure 2) and should have distinguished telomeric repeats, the cell staining image suggested that TR conjugates are superior to Cy3 conjugates for observing telomeres in the cells. Furthermore PI polyamide signals in TH59TR images were slightly stronger than those in deamino TH59TR images, presumably because, as shown in Table 1 as T_m values of not-conjugated polyamides, the former has higher affinities to human telomeric repeats than the latter.

Next, following the previous report,[12] we used immuno-fluorescence to prove that the TH59TR and deamino TH59TR can localize to telomeres. We reasoned that a shelterin complex component in telomeres, TRF1 protein, which binds to
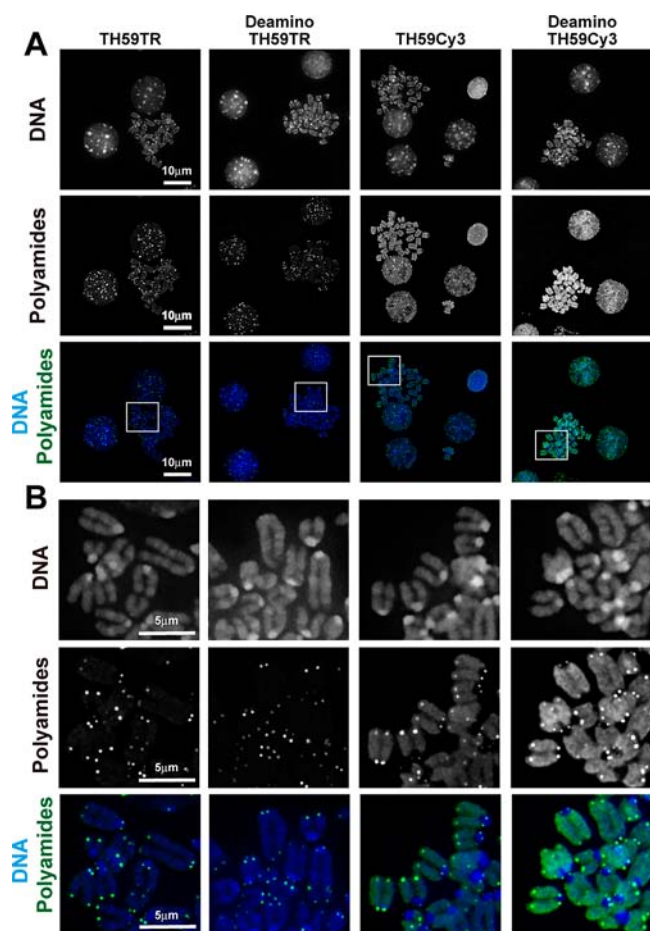
Figure 3. Telomere staining of mouse MC12 cell spreads with fluorescent polyamides. (A) The MC12 spreads were stained with DAPI (first row) and the fluorescent polyamides (second row): first column, TH59TR; second column, deamino TH59TR; third column, TH59Cy3; fourth column, deamino TH59Cy3. The merged images of DAPI and polyamides staining are shown in the third row. Enlarged images of the boxed region in panel (A) are demonstrated in panel (B).
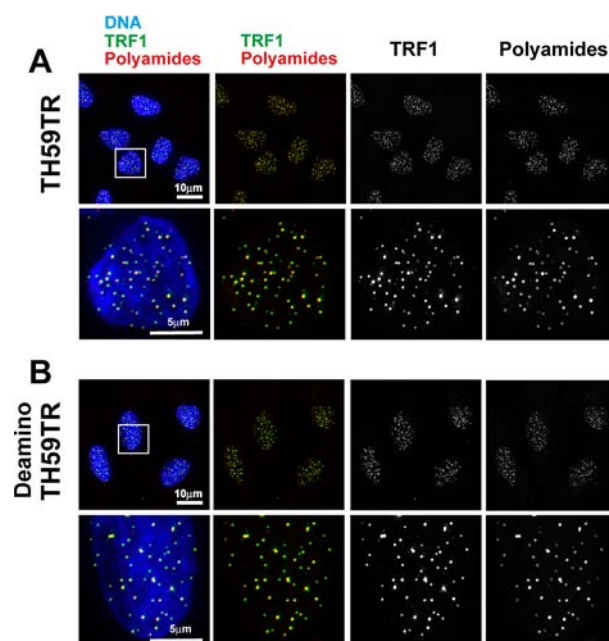

Figure 4. Staining of telomeric repeats with fluorescent polyamides and co-localization with telomere binding protein TRF1. HeLa1.3 cells were stained with DAPI, TRF1 antibody, and TH59TR (A) or deamino TH59TR (B). Enlarged images of the boxed regions in first row images are shown in the second row. Note that TH59TR or deamino TH59TR foci colocalize with immunofluorescence signals with TRF1 antibodies.

TTAGGG repeats and controls telomere length,[2−5] should colocalize with the TH59TR and deamino TH59TR. Figure 4 shows human HeLa cell treated with the TH59TR and deamino TH59TR (red) together with the immunofluorescence signal of TRF1 antibodies (green). This examination suggested that the signals of TH59TR and deamino TH59TR were colocalized with that of TRF1 because the resulting overlapping yellow signals were observed.

Furthermore, TH59TR and TRF1 signals were extracted from the Figure 4A image, and their intensities were compared at a single telomere level. As shown in Figure 5, we found a close correlation at a single telomere level between signals of TH59TR and TRF1-antibody (correlation coefficient: 0.80), suggesting telomere length is highly related to abundance of shelterin complex in telomeres. This finding is a good agreement with the "protein-counting" model of telomere length regulation.[2−5] Various methods of telomere length analysis have been developed, but they require denaturation or electrophoresis steps.[23] These observations demonstrate that TH59TR and deamino TH59TR are telomere-specific polyamide probes that allows us to observe human telomeres

without breaking the telomere structures and to estimate telomere length easily with a simple staining protocol.

Moreover, we examined the effect of the washing process on telomere staining. We detected the telomeric signals without a washing process; however, this process helped reduce the background or nonspecific PI polyamide binding (shown in Figure S7, Supporting Information).

■ CONCLUSION

In this study, we developed a synthetic scheme for tandem hairpin PI polyamides with two units of Fmoc SPPS, which we used to synthesize telomere-targeting polyamides conjugated with TR or Cy3. In mouse and human cells, TR-conjugated polyamides 1 and 2 (TH59TR and deamino TH59TR, respectively) highlighted the telomere foci clearly. This novel method simplifies the synthesis of PI polyamide probes targeting the human telomeric repeat TTAGGG and is useful for methods to label and analyze telomeres in the cells without breaking the telomere structures.

■ MATERIALS AND METHODS

Materials for the Synthesis. ^{1}H NMR spectra were recorded on a JEOL JNM ECA-600 spectrometer (600 MHz for ^{1}H), with chemical shifts reported in parts per million relative to residual solvent and coupling constants in hertz. The following abbreviations were applied to spin multiplicity: s (singlet), d (doublet), t (triplet), q (quartet), and m (multiplet). HPLC analysis was performed on a JASCO Engineering PU-2089 plus series system using 4.6 × 150 mm X-Terra MS C_{18} reversed-phase column in 0.1% TFA in water with acetonitrile as the eluent at a flow rate of 1.0 mL/min and a linear gradient elution of 0 to 100% acetonitrile in 40 min with detection at 254 nm. HPLC purification was performed with a Jasco Engineering UV2075 HPLC UV/vis detector and a PU-2080 plus series system using a 4.6 × 150 mm Chemcobond 5-ODS-H reversed-phase column
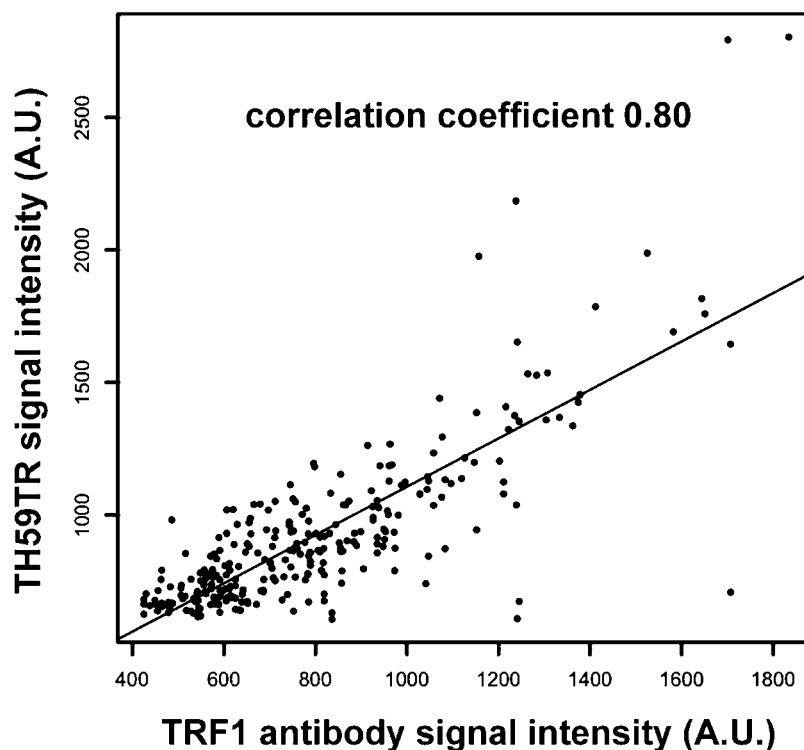
Figure 5. Correlation between signal intensities of TH59TR and immunofluorescence for TRF1. TH59TR and TRF signals were extracted from the Figure 4A image and their intensities were compared at single telomere level and shown as a scattered plot. A.U., arbitrary unit.

in 0.1% TFA in water with acetonitrile as the eluent at a flow rate of 1.0 mL/min and a linear gradient elution of 30 to 75% acetonitrile in 20 min with detection at 254 nm. Collected fractions were analyzed by ESI-TOF-MS (Bruker). For the collect mass measurement, external mass calibration (m/z 622.0290 and 922.0098), purchased from Agilent Technologies, was used. Reversed-phase flash chromatography was performed on CombiFlash Rf (Teledyne Isco, Inc.) using a 4.3 g reversed-phase flash column (C18 RediSep Rf) in 0.1% TFA in water with acetonitrile as the eluent at a flow rate of 18.0 mL/min and a linear gradient elution of 0 to 35% acetonitrile in 5−30 min with detection at 254 nm. DNA oligonucleotides were purchased from Sigma. Fmoc-β-Ala-Wang resin (0.55 mmol/g), Fmoc-mini-PEG-OH, and Fmoc-D-Dab(Boc)-OH were purchased from Peptide International. Fmoc-P-CO$_2$H, Fmoc-PI-CO$_2$H, and DMF used for solid-phase synthesis, 1-methyl-2-pyrrolidone (NMP), trifluoroacetic acid (TFA), and piperidine were from Wako. O-(1H-6-Chlorobenzotriazol-1-yl)-1,1,3,3-tetramethyluronium hexafluorophosphate (HCTU) was from Peptide Institute, Inc. Fmoc-β-Ala-Wang resin, Fmoc-γ-Abu-OH, and PyBOP were from Novabiochem. DIEA was from Nacalai Tesque, Inc. DMF used for solution-phase synthesis was from Kanto Chemical Co., Inc. 3,3′-Diamino-N-methyldipropylamine, 10% Pd/C, and 1-methyl-1H-imidazole-2-carboxylic acid were from Aldrich. TR succinimidyl ester and Cy3-NHS ester were from Molecular Probes. All other solvents and materials were from standard suppliers (highest quality available).

Materials for the Analysis of Spectra and Thermal Denaturation Analysis. Polyamide concentrations were calculated with a Nanodrop ND-1000 spectrophotometer (Thermo Fisher Scientific Inc.) using an extinction coefficient of 9900 M^{-1} cm^{-1} per one pyrrole or imidazole moiety at λ_{max} near 310 nm. UV−vis spectra were measured on a spectophotometer V-650 (JASCO). Steady-state fluorescence spectra were obtained on a spectrofluorometer FP-6300 (JASCO). These two kinds of spectra were obtained at room temperature. Melting temperature analyses were performed on a spectophotometer V-650 (JASCO) equipped with a thermocontrolled PAC-743R cell changer (JASCO) and a refrigerated and heating circulator F25-ED (Julabo).

Synthesis of IIP-CO$_2$Me (6). Compound 6 was synthesized from O$_2$N-IP-CO$_2$Me (5). To a solution of 5 (2001 mg, 6.51 mmol) in MeOH (50 mL) was added 10% Pd/C (100 mg), and the reaction mixture was stirred for 6 h at room temperature under high pressure (0.23 MPa) of hydrogen gas. The reaction mixture was filtered through the filter paper with dichloromethane and concentrated in vacuo to afford 1478 mg of yellow amine crude, which was used in the next coupling without further purification. To a solution of the amine in DMF 25 mL was added a solution of 1-methyl-1H-imidazole-2-carboxylic acid (651 mg, 5.16 mmol) and PyBOP (2685 mg, 5.16 mmol) in DIEA (1.89 mL, 10.9 mmol) and DMF (30 mL), and the reaction mixture was stirred over a weekend. After concentration, the residue was triturated with water as a brown solid. The residue was dissolved in dichloromethane and concentrated in vacuo to afford 6 (1931 mg, 97% yield). The compound was used in the next reaction without further purification: analytical HPLC t_R = 16.0 min; ESI-TOF-MS m/z calcd for C$_{17}$H$_{19}$N$_7$O$_4$ [M + H]$^+$ 386.1577, found 386.1422; ^{1}H NMR (600 MHz, DMSO-d_6) δ 10.49 (s, 1H; NH), 9.78 (s, 1H; NH), 7.57 (s, 1H; CH), 7.53 (d, 1H; J = 1.3 Hz; CH), 7.46 (s, 1H; CH), 7.08 (s, 1H; CH), 7.01 (d, 1H; J = 1.3 Hz; CH), 4.01 (s, 3H; NMe), 4.00 (s, 3H; NMe), 3.83 (s, 3H; NMe), 3.74 (s, 3H; OMe).

Synthesis of IIP-CO$_2$H (7). Compound 7 was synthesized from IIP-CO$_2$Me (6) by hydrolysis. To a solution of 6 (1812 mg, 4.73 mmol) in methanol/water (1:1, total 40 mL) was added sodium hydroxide (2.5 g), and the reaction mixture was stirred for 6 h at 40 °C, as followed by the evaporation of methanol. The base was neutralized by the addition of hydrochloric acid at 0 °C to afford precipitations. The precipitates were dried in vacuo to afford compound 7 (1102 mg, 60% yield) as a brown powder. The compound was used in the next coupling without further purification: analytical HPLC t_R = 13.5 min; ESI-TOF-MS m/z calcd for C$_{16}$H$_{17}$N$_7$O$_4$ [M + H]$^+$ 372.1420, found 372.1440; ^{1}H NMR (600 MHz, DMSO-d_6) δ 10.41 (s, 1H; NH), 9.86 (s, 1H; NH), 7.57 (s, 1H; CH), 7.48 (s, 1H; CH), 7.47 (d, 1H; J = 2.1 Hz; CH), 7.12 (s, 1H; CH), 6.96 (d, 1H; J = 2.0 Hz; CH), 4.01 (s, 3H; NMe), 4.00 (s, 3H; NMe), 3.83 (s, 3H; NMe).

Synthesis of Fmoc-D-Dab(IIP)-OH (9). Compound **9** was synthesized from **7** and Fmoc-D-Dab(Boc)-OH. The procedure for the synthesis is as follows. To remove the Boc group, TFA (487.5 μL) and water (12.5 μL) were added to Dab (100 mg, 0.23 mmol) and mixed until Dab dissolved. After concentration of the mixture, the residue was washed with diethyl ether, triturated with dichloromethane−diethyl ether, and then dried in vacuo. DMF (1 mL) and DIEA (200 μL) were added to the resulting Fmoc-D-Dab(NH$_2$)-OH as a white powder. On the other hand, crude **7** (73 mg, 0.20 mmol) and PyBOP (103 mg, 0.20 mmol) were dissolved in DMF (500 μL) and DIEA (160 μL) and mixed to afford the activated compound **8**. At room temperature, the solution of the compound **8** was added slowly to Fmoc-D-Dab(NH$_2$)-OH solution, and the reaction solution was mixed for 10 min and then settled for 1 h at room temperature. After concentration in vacuo, the residue was washed with diethyl ether and then triturated with water. The resulting residue was dried to allow the compound **9** (134 mg, 98% yield) as a yellow powder. The compound was used in the next solid-phase synthesis without purification: analytical HPLC t_R = 21.3 min; ESI-TOF-MS m/z calcd for C$_{35}$H$_{35}$N$_9$O$_7$ [M + H]$^+$ 694.2738, found 694.2723; ^{1}H NMR (600 MHz, DMSO-d_6), δ 10.28 (s, 1H; NH), 9.74 (s, 1H; NH), 8.06 (t, 1H, J = 5.5 Hz; NH), 7.90 (d, 2H, J = 8.3 Hz; CH × 2), 7.74 (t, 2H, J = 6.5 Hz; CH × 2), 7.72 (d, 1H, J = 8.2 Hz; NH), 7.56 (s, 1H; CH), 7.46 (s, 1H; CH), 7.42 (t, 2H, J = 7.6 Hz; CH × 2), 7.33 (t, 2H, J = 7.6 Hz; CH × 2), 7.22 (d, 1H, J = 1.4 Hz; CH), 7.08 (s, 1H, CH), 6.98 (d, 1H, J = 1.4 Hz; CH), 4.28−4.29 (m, 2H; CH$_2$), 4.23−4.26 (m, 1H; CH), 4.02−4.05 (m, 1H; CH), 4.01 (s, 3H; NMe), 4.00 (s, 3H; NMe), 3.80 (s, 3H; NMe), 2.89−3.08 (m, 2H; CH$_2$), 1.99−2.04 (m, 1H; CH), 1.79−1.85 (m, 1H; CH).

General Procedures of Fmoc Solid-Phase Synthesis. Each synthesis of tandem hairpin PI polyamides (**10, 11**) was performed on a PSSM-8 (Shimadzu) with a computer-assisted operation system on a 0.02 mmol scale (about 40 mg of Fmoc-β-Wang resin, 0.55 mmol/g) by using Fmoc chemistry. An Fmoc unit (0.20 mmol) in each step was set up to solve by NMP (1 mL) on the synthetic line. Fmoc units in each step were as follows: Fmoc-P-CO$_2$H (77 mg), Fmoc-PI-CO$_2$H (70 mg), IIP-CO$_2$H (70 mg) (**7**), Fmoc-D-Dab(IIP)−OH (70 mg) (**9**), Fmoc-mini-PEG-OH (81 mg), and Fmoc-γ-Abu-OH (69 mg). Procedures were as follows: twice deblocking for 4 min with 20% piperidine/DMF (0.5 mL), activating for 2 min with HCTU (88 mg, 0.21 mmol) in DMF (1 mL) and 10% DIEA/DMF (0.4 mL), coupling for 60 min, and washing with DMF. At the last coupling of **11**, a solution of the activated compound **7** (70 mg, 0.19 mmol) with PyBOP (103 mg, 0.20 mmol) in 18% DIEA/NMP 0.91 mL was used. After the last coupling of **10**, the deblocking of amino group at γ-turn was performed. All coupling were carried out with a single-coupling cycle. All lines were purged with solution transfers and bubbled by nitrogen gas for stirring the resin.

Synthesis of IIP-D-Dab-PPPI-PEG-D-Dab(IIP)-PPPI-β-amine (10, TH59). Solid-phase synthesis was performed with 44 mg of resin. After that, the compound supported by Wang resin was cleaved using 3,3′-diamino-N-methyldipropylamine (96% assay). A 0.4 mL portion of that was added, followed by stirring for 3 h at 45 °C. The resin was removed by filtration and washed thoroughly with dichloromethane, and the filtrate was concentrated in vacuo. The residue was washed with diethyl ether, triturated with dichloromethane−diethyl ether, and then dried in vacuo. The resulting crude polyamide (32.0 mg) was purified by reversed-phase flash chromatography, and appropriate fractions were collected under freeze-dry condition to give the compound **10** (3.7 mg, 1.6 × 10^{-3} mmol, 6.9% yield in 10 steps): analytical HPLC t_R = 14.9 min; ESI-TOF-MS m/z calcd for C$_{102}$H$_{127}$N$_{41}$O$_{20}$ [M + 3H]$^{3+}$ 749.6715, found 749.6642.

Synthesis of IIP-γ-PPPI-PEG-D-Dab(IIP)-PPPI-β-amine (11, deamino TH59). Solid-phase synthesis was performed with 44 mg resin. After solid-phase synthesis and similar cleavage, the crude compound **11** was gained according to the above procedure. The resulting crude polyamide (22.0 mg) was purified similarly to give the compound **11** (5.5 mg, 2.5 × 10^{-3} mmol, 10% yield in 11 steps): analytical HPLC t_R = 16.0 min; ESI-TOF-MS m/z calcd for C$_{102}$H$_{126}$N$_{40}$O$_{20}$ [M + 3H]$^{3+}$ 744.6769, found 744.6678.

Synthesis of the Conjugate 1 (TH59TR). First TR succinimidyl ester (1.0 mg) in DMF (80 μL) was prepared. Compound **10** (0.8 mg, 3.6 × 10^{-4} mmol) was dissolved in DMF (199.8 μL) and DIEA (0.2 μL), and the solution of TR succinimidyl ester (48 μL, 7.4 × 10^{-4} mmol) was added to that of **10**, followed by mixing for 4 h at room temperature with shielding the light. The reaction mixture was purified by reversed-phase HPLC, and appropriate fractions were collected under freeze-dry conditions to give the compound **1** (0.4 mg) as a blue powder: analytical HPLC t_R = 19.4 min; ESI-TOF-MS m/z calcd for C$_{139}$H$_{166}$N$_{44}$O$_{27}$S$_2$ [M + 3H]$^{3+}$ 983.4215, found 983.3976.

Synthesis of the Conjugate 2 (Deamino TH59TR). Compound **11** (0.6 mg, 2.7 × 10^{-4} mmol) and the powdered TR succinimidyl ester (0.3 mg, 3.7 × 10^{-4} mmol) were dissolved in DMF (200 μL) and DIEA (4 μL), followed by mixing for 4 h at room temperature with shielding the light. The reaction mixture was purified as described above to give the compound **2** (0.8 mg) as a blue powder: analytical HPLC t_R = 20.7 min; ESI-TOF-MS m/z calcd for C$_{139}$H$_{165}$N$_{43}$O$_{27}$S$_2$ [M + 3H]$^{3+}$ 978.4179, found 978.3985.

Synthesis of the Conjugate 3 (TH59Cy3). First Cy3-NHS ester (4 mg) in DMF (80 μL) was prepared. The compound **10** (1.0 mg, 4.4 × 10^{-4} mmol) was dissolved in DMF (199.8 μL) and DIEA (0.2 μL), and the solution of Cy3-NHS ester (20.4 μL, 1.3 × 10^{-3} mmol) was added to that of **10**, followed by mixing for 4 h at room temperature with shielding of light. The reaction mixture was purified as described above to give the compound **3** (1.6 mg) as a red powder: analytical HPLC t_R = 19.2 min; ESI-TOF-MS m/z calcd for C$_{132}$H$_{162}$N$_{43}$O$_{21}^+$ [M + 2H]$^{3+}$ 895.7694, found 895.7559.

Synthesis of the Conjugate 4 (Deamino TH59Cy3). Compound **11** (0.9 mg, 4.0 × 10^{-4} mmol) was dissolved in DMF (180 μL) and DIEA (20 μL), and the solution of Cy3-NHS ester (40 μL, 2.6 × 10^{-3} mmol.) was added to that of **11**, followed by mixing for 5 h at room temperature with shielding the light. The reaction mixture was purified as described above to give the compound **4** (1.5 mg) as a red powder: analytical HPLC t_R = 20.5 min; ESI-TOF-MS m/z calcd for C$_{132}$H$_{161}$N$_{42}$O$_{21}^+$ [M + 2H]$^{3+}$ 890.7657 found 890.7651.

Telomere Staining. *Materials for Telomere Staining.* Cell images were recorded with DeltaVision (Applied Precision). Mouse MC12 cells were gifts from Dr. Kimura, Osaka University. Hela1.3 cells were generous gifts of Dr T. de Lange (Rockefeller University). DMEM medium was purchased from Life technology. Normal goat serum (NGS) was from Millipore. Nocodazole, paraphenylene diamine, and Triton X-100 were from Sigma. NaBH$_4$ was from Fluka. DAPI was from Roche. Rabbit anti-TRF1 antibody was a generous gift of Dr. F. Ishikawa (Kyoto University). Secondary antibody (goat anti4rabbit Alexa 488) was from Molecular Probes. All other materials were from standard suppliers (highest quality available).

Telomere Staining of Mouse MC12 Cell Spreads with Fluorescent Polyamides.[24] Mouse MC12 cells were maintained in DMEM medium containing 10% fetal bovine serum (FBS) at 37 °C (5% CO$_2$). Mouse MC12 cells were blocked mitotically by adding 0.1 μg/mL nocodazole for 1 h. The cells were swollen by treatment with a hypotonic buffer (0.075 M KCl) for 15 min at room temperature, fixed with a methanol/acetic acid (3:1) solution for 5 min. After centrifugation, cell pellet was again suspended in the methanol/acetic acid solution. The cell suspension was spread on coverslips and air-dried for 30 min. The cell spread coverslips were kept at 4 °C until use.

The air-dried spread coverslips were soaked in TEN buffer (10 mM Tris-HCl, pH7.5, 1 mM EDTA and 100 mM NaCl) overnight at 4 °C before use. For blocking, the spread coverslips were treated with 10% NGS in TEN buffer for 30 min at room temperature. After brief washing with TE buffer (10 mM Tris-HCl, pH7.5, 1 mM EDTA), the spread coverslips were incubated with 10% NGS, 500 nM polyamides and 0.5 μg/mL DAPI in TE buffer for 1 h at room temperature. After washing with TEN buffer (five times for 3 min), the spread coverslips were mounted in PPDI solution [10 mM HEPES pH 7.5, 100 mM KCl, 1 mM MgCl$_2$, 80% glycerol, 1 mg/mL paraphenylene diamine], and the coverslips were sealed with a nail polish. Sectioning images were recorded with DeltaVision and deconvoluted to eliminate "out-

of-focus" blur.[25,26] The deconvoluted images were projected to obtain the maximum intensity ('Quick Projection' tool) of telomeric signals.

Co-localization of the Signal of Telomere-Specific Polyamides and TRF1. HeLa1.3 cells were maintained at 37 °C (5% CO_2) in DMEM containing 10% FBS. For polyamide staining, the HeLa cells were grown on coverslips coated with polylysine. The cell coverslips were washed in phosphate-buffered saline (PBS) and fixed with 2% formaldehyde in PBS for 15 min at room temperature. The fixed cell coverslips were then treated with 0.5 mg/mL $NaBH_4$ in PBS for 10 min, rinsed with PBS (twice for 5 min), and permeabilized with 0.5% Triton X-100 in PBS. After washing with PBS twice, the coverslips were kept at 4 °C for storage. For fixation process, when we used XBE2 buffer (10 mM HEPES pH 7.5, 2 mM $MgCl_2$, 100 mM KCl, 5 mM EGTA) as described in ref 12 and 26, instead of PBS, a similar telomere staining result was obtained (data not shown).

For blocking, the cell coverslips were treated with 10% NGS in TE buffer for 30 min at room temperature. After a brief rinse with TE buffer, the cells were incubated with 10% NGS, rabbit anti-TRF1 antibody, 500 nM polyamide in DMF, and 0.5 μg/mL DAPI in TE buffer at 37 °C for 1 h. After washing with TEN200 (10 mM Tris-HCl, pH7.5, 1 mM EDTA and 200 mM NaCl) (five times for 3 min), the cells were incubated with secondary antibody (500-fold diluted goat antirabbit Alexa 488) and 1% NGS in TEN buffer for 1 h, and followed by five washes (3 min) with TEN200. The mounting and subsequent image acquisitions were performed as described above. Tight cross-linking by fresh formaldehyde solution tended to prevent the telomere staining. In such case, incubation of the fixed cells 37 °C overnight facilitated the telomere staining (not shown).

For comparison between the TH59TR and TRF1-antibody signals, they were extracted from the Figure 4A image as described previously.[12] The telomere signals yielded by the anti-TRF1 antibody and TH59TR were extracted based on threshold values using the Softworks software (Applied Precision). The maximum intensity values of Alexa 488 (anti-TRF1 antibody) and Texas Red signals in the extracted telomere regions were then used as telomere signals. Note that the mean values of Alexa 488 (anti-TRF1 antibody) and Texas Red signals in the extracted telomere regions also produced a similar correlation to Figure 5 (not shown). Intensities of the corresponding TH59TR and TRF1-antibody signals were compared and shown as a scattered plot. Correlation coefficient was calculated using R software.

ASSOCIATED CONTENT

Ⓢ Supporting Information

Mass spectra of the compounds **1−4**, **10**, **11**, thermal denaturation profiles of the compounds **10** and **11**, washing effect on the telomere staining. This information is available free of charge via the Internet at http://pubs.acs.org.

AUTHOR INFORMATION

Corresponding Authors

bando@kuchem.kyoto-u.ac.jp
hs@kuchem.kyoto-u.ac.jp
kmaeshim@nig.ac.jp

Notes

The authors declare no competing financial interest.

ACKNOWLEDGMENTS

REFERENCES

(1) Blackburn, E. H. *Angew. Chem., Int. Ed.* **2010**, *49*, 7405−7421.
(2) Nandakumar, J.; Cech, T. R. *Nat. Rev. Mol. Cell Biol.* **2013**, *14*, 69−82.
(3) Zakian, V. A. *Exp. Cell Res.* **2012**, *318*, 1456−1460.
(4) Smogorzewska, A.; de Lange, T. *Annu. Rev. Biochem.* **2004**, *73*, 177−208.
(5) Smogorzewska, A.; van Steensel, B.; Bianchi, A.; Oelmann, S.; Schaefer, M. R.; Schnapp, G.; de Lange, T. *Mol. Cell. Biol.* **2000**, *20*, 1659−1668.
(6) (a) Dervan, P. B. *Bioorg. Med. Chem.* **2001**, *9*, 2215−2235. (b) Dervan, P. B.; Edelson, B. S. *Curr. Opin. Struct. Biol.* **2003**, *13*, 284−299. (c) Dervan, P. B.; Doss, R. M.; Marques, M. A. *Curr. Med. Chem.: Anti-Cancer Agents* **2005**, *5*, 373−387. (d) Blackledge, M. S.; Melander, C. *Bioorg. Med. Chem.* **2013**, *21*, 6101−6114.
(7) White, S.; Szewczyk, J. W.; Turner, J. M.; Baird, E. E.; Dervan, P. B. *Nature* **1998**, *391*, 468−471.
(8) (a) Turner, J. M.; Swalley, S. E.; Baird, E. E.; Dervan, P. B. *J. Am. Chem. Soc.* **1998**, *120*, 6219−6226. (b) Wang, C. C.; Ellervik, U.; Dervan, P. B. *Bioorg. Med. Chem.* **2001**, *9*, 653−657.
(9) (a) de Clairac, R. P. L.; Geierstanger, B. H.; Mrksich, M.; Dervan, P. B.; Wemmer, D. E. *J. Am. Chem. Soc.* **1997**, *119*, 7909−7916. (b) Murty, M. S. R. C.; Sugiyama, H. *Biol. Pharm. Bull.* **2004**, *27*, 468−474.
(10) (a) Herman, D. M.; Turner, J. M.; Baird, E. E.; Dervan, P. B. *J. Am. Chem. Soc.* **1999**, *121*, 1121−1129. (b) Melander, C.; Herman, D. M.; Dervan, P. B. *Chem.—Eur. J.* **2000**, *6*, 4487−4497. (c) Morinaga, H.; Bando, T.; Takagaki, T.; Yamamoto, H.; Hashiya, K.; Sugiyama, H. *J. Am. Chem. Soc.* **2011**, *133*, 18924−18930. (d) Li, B. C.; Montgomery, D. C.; Puckett, J. W.; Dervan, P. B. *J. Org. Chem.* **2013**, *78*, 124−133.
(11) (a) Herman, D. M.; Baird, E. E.; Dervan, P. B. *Chem.—Eur. J.* **1999**, *5*, 975−983. (b) Kers, I.; Dervan, P. B. *Bioorg. Med. Chem.* **2002**, *10*, 3339−3349. (c) Schaal, T. D.; Mallet, W. G.; McMinn, D. L.; Nguyen, N. V.; Sopko, M. M.; John, S.; Parekh, B. S. *Nucleic Acids Res.* **2003**, *31*, 1282−1291. (d) Sasaki, S.; Bando, T.; Minoshima, M.; Shinohara, K.; Sugiyama, H. *Chem.—Eur. J.* **2008**, *14*, 864−870.
(12) Maeshima, K.; Janssen, S.; Laemmli, U. K. *EMBO J.* **2001**, *20*, 3218−3228.
(13) (a) Bando, T.; Narita, A.; Saito, I.; Sugiyama, H. *J. Am. Chem. Soc.* **2003**, *125*, 3471−3485. (b) Bando, T.; Sugiyama, H. *Acc. Chem. Res.* **2006**, *39*, 935−944. (c) Bando, T.; Sasaki, S.; Minoshima, M.; Dohno, C.; Shinohara, K.; Narita, A.; Sugiyama, H. *Bioconjugate Chem.* **2006**, *17*, 715−720. (d) Takagaki, T.; Bando, T.; Sugiyama, H. *J. Am. Chem. Soc.* **2012**, *134*, 13074−13081.
(14) (a) Vaijayanthi, T.; Bando, T.; Pandian, G. N.; Sugiyama, H. *ChemBioChem* **2012**, *13*, 2170−2185. (b) Vaijayanthi, T.; Bando, T.; Hashiya, K.; Pandian, G. N.; Sugiyama, H. *Bioorg. Med. Chem.* **2013**, *21*, 852−855. (c) Su, W.; Bagshaw, C. R.; Burley, G. A. *Sci. Rep.* **2013**, *3*, 1883.
(15) (a) Ohtsuki, A.; Kimura, M. T.; Minoshima, M.; Suzuki, T.; Ikeda, M.; Bando, T.; Nagase, H.; Shinohara, K.; Sugiyama, H. *Tetrahedron Lett.* **2009**, *50*, 7288−7292. (b) Pandian, G. N.; Shinohara, K.; Ohtsuki, A.; Nakano, Y.; Minoshima, M.; Bando, T.; Nagase, H.; Yamada, Y.; Watanabe, A.; Terada, N.; Sato, S.; Morinaga, H.; Sugiyama, H. *ChemBioChem* **2011**, *12*, 2822−2828. (c) Pandian, G. N.; Ohtsuki, A.; Bando, T.; Sato, S.; Hashiya, K.; Sugiyama, H. *Bioorg. Med. Chem.* **2012**, *20*, 2656−2660. (d) Pandian, G. N.; Nakano, Y.; Sato, S.; Morinaga, H.; Bando, T.; Nagase, H.; Sugiyama, H. *Sci. Rep.* **2012**, *2*, 544.
(16) Fujimoto, J.; Bando, T.; Minoshima, M.; Kashiwazaki, G.; Nishijima, S.; Shinohara, K.; Sugiyama, H. *Bioorg. Med. Chem.* **2008**, *16*, 9741−9744.
(17) (a) Takahashi, R.; Bando, T.; Sugiyama, H. *Bioorg. Med. Chem.* **2003**, *11*, 2503−2509. (b) Sasaki, S.; Bando, T.; Minoshima, M.; Shimizu, T.; Shinohara, K.; Takaoka, T.; Sugiyama, H. *J. Am. Chem. Soc.* **2006**, *128*, 12162−12168. (c) Kashiwazaki, G.; Bando, T.; Shinohara, K.; Minoshima, M.; Nishijima, S.; Sugiyama, S. *Bioorg. Med. Chem.* **2009**, *17*, 1393−1397. (d) Kashiwazaki, G.; Bando, T.;

Shinohara, K.; Minoshima, M.; Kumamoto, H.; Nishijima, S.; Sugiyama, H. *Bioorg. Med. Chem.* **2010**, *18*, 2887−2893.

(18) Wurtz, N. R.; Turner, J. M.; Baird, E. E.; Dervan, P. B. *Org. Lett.* **2001**, *3*, 1201−1203.

(19) (a) Rucker, V. C.; Foister, S.; Melander, C.; Dervan, P. B. *J. Am. Chem. Soc.* **2003**, *125*, 1195−1202. (b) Rucker, V. C.; Dunn, A. R.; Sharma, S.; Dervan, P. B.; Gray, H. B. *J. Phys. Chem. B* **2004**, *108*, 7490−7494.

(20) (a) Pilch, D. S.; Poklar, N.; Gelfand, C. A.; Law, S. M.; Breslauer, K. J.; Baird, E. E.; Dervan, P. B. *Proc. Natl. Acad. Sci. U.S.A.* **1996**, *93*, 8306−8311. (b) Muzikar, K. A.; Meier, J. L.; Gubler, D. A.; Raskatov, J. A.; Dervan, P. B. *Org. Lett.* **2011**, *13*, 5612−5615.

(21) Kumar, S.; Xue, L.; Arya, D. P. *J. Am. Chem. Soc.* **2011**, *133*, 7361−7375.

(22) (a) Herman, D. M.; Baird, E. E.; Dervan, P. B. *J. Am. Chem. Soc.* **1998**, *120*, 1382−1391. (b) Dose, C.; Farkas, M. E.; Chenoweth, D. M.; Dervan, P. B. *J. Am. Chem. Soc.* **2008**, *130*, 6859−6866.

(23) Aubert, G.; Hills, M.; Lansdorp, P. M. *Mutat. Res.* **2012**, *730*, 59−67.

(24) Yoshida, I. *Cytogenet. Genome Res.* **2002**, *99*, 44−51.

(25) Maeshima, K.; Laemmli, U. K. *Dev. Cell* **2003**, *4*, 467−80.

(26) Maeshima, K.; Yahata, K.; Sasaki, Y.; Nakatomi, R.; Tachibana, T.; Hashikawa, T.; Imamoto, F.; Imamoto, N. *J. Cell Sci.* **2006**, *119*, 4442−51.